Am J Physiol Cell Physiol 286: C893–C904, 2004;
10.1152/ajpcell.00127.2003.

Rat cerebellar granule cells are protected from glutamate-induced excitotoxicity by *S*-nitrosoglutathione but not glutathione

Chung-Yu Li, Ting-Yu Chin, and Sheau-Huei Chueh
Department of Biochemistry, National Defense Medical Center, Taipei 114, Taiwan, Republic of China

Submitted 3 April 2003; accepted in final form 20 November 2003

Li, Chung-Yu, Ting-Yu Chin, and Sheau-Huei Chueh. Rat cerebellar granule cells are protected from glutamate-induced excitotoxicity by *S*-nitrosoglutathione but not glutathione. *Am J Physiol Cell Physiol* 286: C893–C904, 2004; 10.1152/ajpcell.00127.2003.—In cultured rat cerebellar granule cells, glutamate or *N*-methyl-D-aspartate (NMDA) activation of the NMDA receptor caused a sustained increase in cytosolic Ca^{2+} levels ($[Ca^{2+}]_i$), reactive oxygen species (ROS) generation, and cell death (respective EC_{50} values for glutamate were 12, 30, and 38 μM) but no increase in caspase-3 activity. Removal of extracellular Ca^{2+} blocked all three glutamate-induced effects, whereas pretreatment with an ROS scavenger inhibited glutamate-induced cell death but had no effect on the $[Ca^{2+}]_i$ increase. This indicates that glutamate-induced cell death is attributable to $[Ca^{2+}]_i$ increase and ROS generation, and the $[Ca^{2+}]_i$ increase precedes ROS generation. Apoptotic cell death was not seen until 24 h after exposure of cells to glutamate. *S*-nitrosoglutathione abolished glutamate-induced ROS generation and cell death, and only a transient $[Ca^{2+}]_i$ increase was seen; similar results were observed with another nitric oxide (NO) donor, *S*-nitroso-*N*-acetylpenicillamine, but not with glutathione, which suggests that the effects were caused by NO. The transient $[Ca^{2+}]_i$ increase and the abolishment of ROS generation induced by glutamate and *S*-nitrosoglutathione were still seen in the presence of an ROS scavenger. Glial cells, which were present in the cultures used, showed no $[Ca^{2+}]_i$ increase in the presence of glutamate, and glutamate-induced granule cell death was independent of the percentage of glial cells. In conclusion, NO donors protect cultured cerebellar granule cells from glutamate-induced cell death, which is mediated by ROS generated by a sustained $[Ca^{2+}]_i$ increase, and glial cells provide negligible protection against glutamate-induced excitotoxicity.

cytosolic calcium concentration; *N*-methyl-D-aspartate; reactive oxygen species

IT HAS BEEN CLEARLY ESTABLISHED that prolonged stimulation with the excitatory neurotransmitter glutamate causes neurological disorders (9, 11). Many cellular processes including increased cytosolic Ca^{2+} concentration ($[Ca^{2+}]_i$), activation of caspases, production of nitric oxide (NO), and generation of reactive oxygen species (ROS), have been reported to contribute to the development of glutamate-induced excitotoxicity (13, 15, 17, 40, 42). However, the essential components and the complete molecular and biochemical pathways involved have not been completely elucidated. Glutamate receptors can be divided into metabotropic and ionotropic receptors, and the latter can be subdivided into *N*-methyl-D-aspartate (NMDA) receptors, α-amino-3-hydroxy-5-methylisoxazole-4-propionic acid (AMPA) receptors, and kainate receptors. It is believed that the initial event in glutamate-induced excitotoxicity is Ca^{2+} influx induced by the activation of NMDA and AMPA receptors (6, 31). The Ca^{2+} overload subsequently results not only in mitochondrial depolarization but also in ROS production (9, 15, 26, 40).

Recently, evidence has been obtained to show that the activity of channels for Ca^{2+} and other ions in the plasma membrane or intracellular organelles is regulated by thiol nitrosylation; this is the case for L-type Ca^{2+} channels (3), cyclic nucleotide-gated cation channels (1, 2), NMDA receptors (30), and ryanodine receptors (46). With the exception of NMDA receptors, nitrosylation of sulfhydryl groups results in channel activation. The role of NO-producing neurons is paradoxical: in the presence of the superoxide anion, the NO generated after NMDA-receptor activation is converted to peroxynitrite, which is believed to cause neurotoxicity (13); however, *S*-nitrosylation of NMDA-receptor thiol groups in the presence of NO results in channel inactivation and, in this case, NO is neuroprotective (27, 30, 41).

One of the main aims of the present study was to use primary cultures of cerebellar granule neurons to elucidate the sequence of events in NMDA-induced cell death and determine the connection between the $[Ca^{2+}]_i$ increase and possible cellular mediators. In addition, we investigated the protective mechanisms involved in glutamate-induced excitotoxicity, which might have clinical significance for neuroprotection. We found that after activation of the NMDA receptor, granule neurons died through a Ca^{2+}-mediated process, and the glutamate-induced cytotoxicity was attributable to the generation of ROS. Glutamate-induced ROS generation was dependent on a sustained $[Ca^{2+}]_i$ increase, which is normally seen in granule cells after NMDA-receptor activation. In the presence of *S*-nitrosoglutathione (GSNO) but not glutathione (GSH), glutamate caused a transient $[Ca^{2+}]_i$ increase but no ROS generation or cell death, and this phenomenon was not affected by the simultaneous addition of a free-radical scavenger. Thus we provide evidence for a direct connection between the sustained $[Ca^{2+}]_i$ increase and ROS generation. Although granule cells are NO-producing neurons (25), it is possible that under our experimental conditions, the amount of endogenously generated NO was insufficient to modify the NMDA receptor.

MATERIALS AND METHODS

Materials

Basal Eagle's medium, fetal bovine serum, glutamine, and penicillin-streptomycin were purchased from Life Technologies (Grand Island, NY). Fura-2 acetoxymethyl ester (AM) and 2′,7′-dichlorodihydrofluorescein diacetate (H_2DCFDA) were obtained from Molecu-

Address for reprint requests and other correspondence: S.-H. Chueh, Dept. of Biochemistry, National Defense Medical Center, 161, Section 6, Min-Chuan East Rd., Taipei 114, Taiwan, Republic of China (E-mail: shch@mail.ndmctsgh.edu.tw).

The costs of publication of this article were defrayed in part by the payment of page charges. The article must therefore be hereby marked "*advertisement*" in accordance with 18 U.S.C. Section 1734 solely to indicate this fact.

lar Probes (Eugene, OR). Manganese (III) tetrakis(1-methyl-4-pyridyl)porphyrin (MnTMPyP) was obtained from Calbiochem (San Diego, CA). Glutamate, NMDA, ATP, carbonyl cyanide *p*-trichloromethoxyphenylhydrazone (CCCP), poly-L-lysine, trypsin, DNase, GSH, GSNO, cytosine arabinoside, Hoechst 33258, and 3-(4,5-dimethylthiazol-2-yl)-2,5-diphenyltetrazolium bromide (MTT) were purchased from Sigma (St. Louis, MO). *S*-nitroso-*N*-acetylpenicillamine (SNAP), MK-801, 6-cyano-7-nitroquinoxaline-2,3-dione (CNQX), and α-methyl-4-carboxyphenylglycine (MCPG) were purchased from Research Biochemicals International (Natick, MA). The caspase-1, -3, and -8 assay kits were purchased from Calbiochem, Pharmingen (San Diego, CA), and Oncogene Research Products (Boston, MA), respectively. All other chemicals were of analytical grade and were obtained from Merck (Darmstadt, Germany).

Cell Cultures

Primary cultures of rat cerebellar granule cells were prepared from 7-day-old Sprague-Dawley rat cerebella as previously described (18). All procedures employing experimental rats were performed in compliance with the guidelines of the Institutional Animal Care and Use Committee of the National Defense Medical Center and Triservice General Hospital, Taiwan. Briefly, Sprague-Dawley rat pups were decapitated and cerebella were isolated and immersed in ice-cold PBS. The cells were dissociated in Ca^{2+}-free buffer that contained 0.25 mg/ml trypsin and 2,400 U/ml DNase and were collected by centrifugation before being plated on poly-L-lysine (20 μg/ml)-coated 24-mm glass coverslips (2×10^6 cells/coverslip) for $[Ca^{2+}]_i$ measurements, 24-well plates (5×10^5 cells/well) for lactate dehydrogenase (LDH) release and MTT assays, or 60-mm dishes (6×10^6 cells/dish) for measurement of caspase activity and ROS generation and were grown in a humidified atmosphere of 5% CO_2-95% air at 37°C. The growth medium consisted of basal Eagle's medium supplemented with 10% fetal bovine serum, 2 mM glutamine, 21.5 mM KCl, 100 U/ml penicillin, and 100 μg/ml streptomycin. Normally, 10 μM cytosine arabinoside was added to cultures 24 h after plating to minimize glial cell proliferation; in some experiments, to obtain a higher percentage of glial cells in the cultures, the concentration was reduced to 5 μM or zero, and the KCl supplement was removed from the medium. Glial cells were identified by positive immunocytochemical staining for glial fibrillary acidic protein and their distinct morphology (see Fig. 10). Experiments were performed on cells grown for 8–10 days after plating.

$[Ca^{2+}]_i$ Measurement

We measured $[Ca^{2+}]_i$ using the fluorescent indicator fura-2 as described previously (10). Briefly, cells grown on glass coverslips were loaded with fura-2 by incubation for 20 min at 37°C with 5 μM fura-2 AM in loading buffer that consisted of (in mM) 150 NaCl, 5 KCl, 5 glucose, 2.2 $CaCl_2$, 1 $MgCl_2$, and 10 HEPES; pH 7.4. The coverslips were then mounted in a modified Cunningham chamber (12) attached to the stage of a Nikon Diaphot inverted microscope that was equipped with a Nikon ×40 Fluor objective, and the fluorescence of the cells was monitored using a dual-excitation spectrofluorometer with a photomultiplier-based detection system (Spex Industries, Edison, NJ). Using a pinhole diaphragm placed in the image plane in front of the photomultiplier, two or three cells were selected per coverslip and excited alternately with 340- or 380-nm light; the emitted fluorescent light was collected via the objective through a 510-nm long wave-pass filter. The $[Ca^{2+}]_i$ was calculated from the ratio of the fluorescence at 340 and 380 nm using the equation described by Grynkiewicz et al. (20) with a K_d of 135 nM and the following parameters obtained on our instrument for fura-2 in granule cells: the ratio of fluorescence at 340-nm to 380-nm wavelength at zero Ca^{2+} concentration, S_{f1}/S_{f2} (designated R_{min}), 0.76; the ratio of fluorescence at 340-nm to 380-nm wavelength at saturating Ca^{2+} concentration, S_{b1}/S_{b2} (designated R_{max}), 2.69; and the ratio of fluorescence at zero Ca^{2+} concentration to saturating Ca^{2+} concentration at 380-nm wavelength, S_{f2}/S_{b2}, 2.33. The results of one representative experiment are illustrated in Figs. 1, 2, 5, 6, and 9, and the means ± SE for the $[Ca^{2+}]_i$ changes, calculated for *n* experiments using different batches of cells, are given in the text.

Treatment of Cultures

Unless otherwise stated, to detect maximal NMDA-receptor activity, Mg^{2+} was removed from the loading buffer during the glutamate stimulation period to avoid Mg^{2+}-dependent block of the NMDA receptor (32, 37), and 10 μM glycine, which is an NMDA-receptor coagonist (21, 33), was added. After two washes with loading buffer, the cells were stimulated for 30 min at room temperature with the indicated concentrations of glutamate or NMDA (1–1,000 μM) in the presence or absence of the test compounds. After an additional two washes, the cells were transferred to serum-free medium and incubated for 4 h at 37°C. Cells were then tested for cell death, ROS generation, and caspase activity. In some experiments (see Fig. 4*E*), cells were incubated for 24 h at 37°C before assay. As controls for these three assays, cells were treated identically except that the glutamate or NMDA was omitted.

Cytotoxicity Tests

Cytotoxicity was quantified by measuring the activity of LDH released from the cells into the medium (24), and neuronal survival was quantified spectrophotometrically using MTT (Ref. 34; see below). Control cells underwent the same treatment except for the addition of glutamate. In some experiments, extracellular Ca^{2+} was omitted from the loading buffer.

MTT assay. MTT reduction was determined as described by Mosmann (34). Briefly, cells in 24-well plates were treated with glutamate for 30 min and incubated in 200 μl of serum-free medium for 4 h, then 20 μl of MTT (5 mg/ml) was added to each well. After incubation at 37°C for 1 h, the blue formazan reduction product produced due to the action of mitochondrial succinate dehydrogenase in living cells but not in dead cells or their lytic debris was dissolved in isopropanol and measured on an ELISA plate reader at 570 nm. Cell survival was expressed as a percentage of that of controls. The data presented are means ± SE for *n* independent experiments using different batches of cells.

LDH determination. The activity of LDH released by damaged cells into the medium was measured as described by Koh and Choi (24). Cells in 24-well plates were treated with glutamate for 30 min and incubated in 200 μl of serum-free medium for 4 h, then a 150-μl aliquot was removed and mixed with 1.5 ml of loading buffer that contained 100 μM NADH and 750 μM pyruvate. The absorbance at 340 nm was monitored for 3 min. Basal LDH release values from control cells not treated with glutamate were determined in each experiment, and the LDH release from treated cells is expressed as a percentage of that from control cells. The data presented are means ± SE for *n* independent experiments using different batches of cells.

Determination of Percentage of Apoptotic Cells

The chromatin-specific dye Hoechst 33258 was used to observe nuclear changes that occur during the process of apoptosis as described previously (7). Briefly, after the indicated treatments, cells grown on coverslips were fixed and stained for 20 min at room temperature with 10 μM Hoechst 33258 in loading buffer. The nuclear morphology was then examined on an Olympus IX-70 fluorescence microscope with excitation and emission wavelengths of 350 and 460 nm, respectively. Apoptotic and nonapoptotic nuclei were counted in 10 randomly chosen fields per coverslip. The percentage of apoptotic cells was expressed as the mean ± SE for six experiments.

Measurement of ROS

Formation of intracellular ROS was measured using H_2DCFDA as described previously (5). The deesterification product H_2DCF, which

is cleaved by esterase, remains trapped within the cells and is readily oxidized to fluorogenic DCF by intracellular ROS. Thus the emission fluorescence increase at 525 nm that is associated with oxidation reflects the intracellular ROS level. Cells grown in 60-mm dishes were treated with glutamate for 30 min and incubated in serum-free medium for 4 h. Cells were then incubated with 100 μM H_2DCFDA for 20 min at 37°C, washed, and collected by gentle scraping with a rubber policeman, and the cellular fluorescence was measured using a spectrofluorometer (Spex Industries). The emission fluorescence spectrum was scanned between 500 and 560 nm using an excitation wavelength of 500 nm. ROS formation was expressed as fluorescence intensity (in arbitrary units) in both control and glutamate-treated cells. Experiments were repeated at least six times using different batches of cells. The results of one representative experiment are illustrated in the figures. In some experiments, the means ± SE values for the fluorescence peak changes, which were calculated for *n* experiments, are also shown.

Caspase Assays

Caspase-3 activity was measured using a caspase-3 assay kit according to the manufacturer's instructions. Briefly, cells grown in 60-mm dishes were treated with glutamate for 30 min and incubated in serum-free medium for 4 h. They were then detached and lysed for

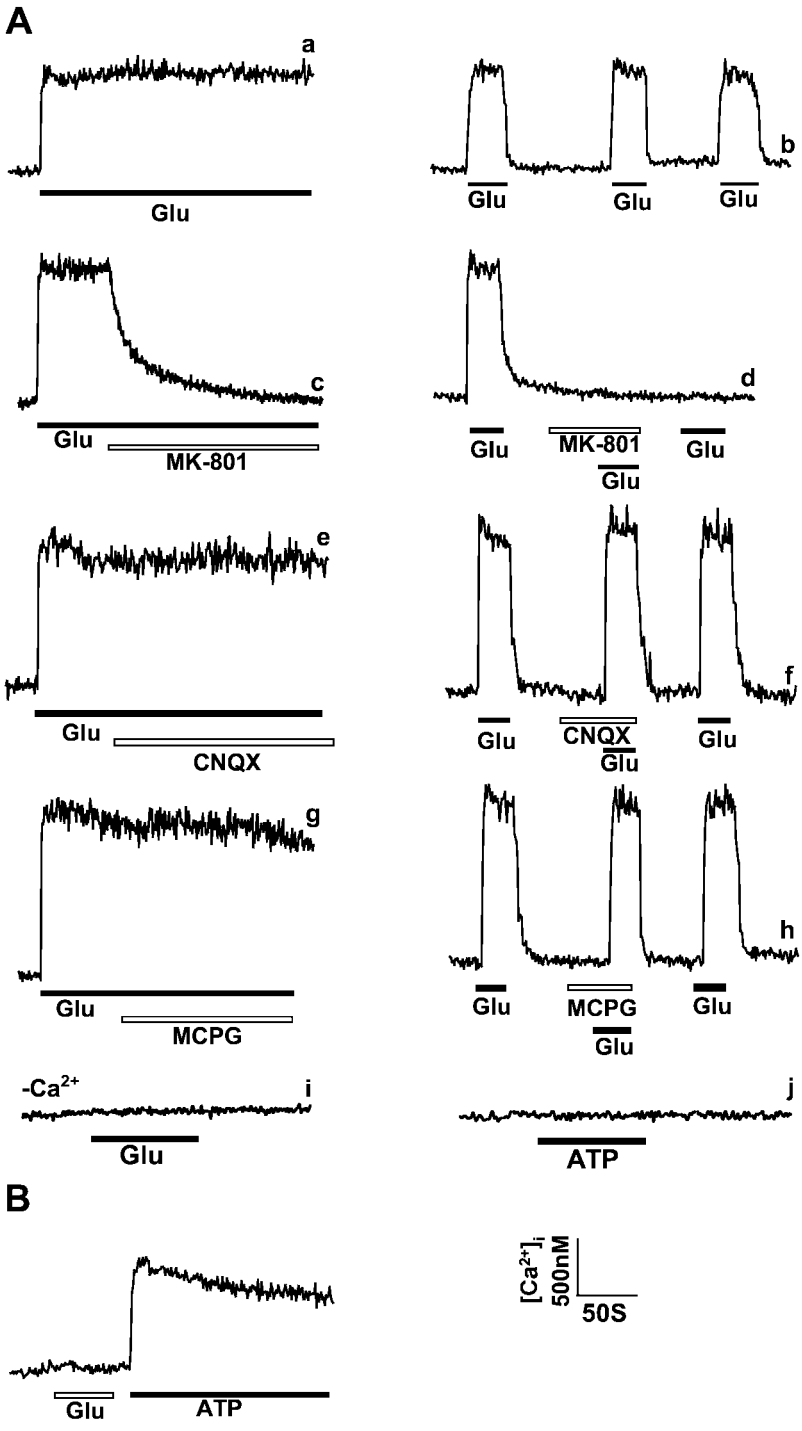

Fig. 1. Glutamate-induced changes in the cytosolic Ca^{2+} concentration ($[Ca^{2+}]_i$) in cerebellar granule cells and non-neuronal cells. *A*: $[Ca^{2+}]_i$ changes in fura-2-loaded granule cells were measured in response to single (*traces a, c, e, g,* and *i*) or repetitive (*traces b, d, f,* and *h*) stimulation with 100 μM glutamate (Glu) or single stimulation with 100 μM ATP (*trace j*) as indicated by the solid horizontal bars. In *traces c-h*, 10 μM MK-801 (*traces c* and *d*), 10 μM 6-cyano-7-nitroquinoxaline-2,3-dione (CNQX, *traces e* and *f*), or 1 mM α-methyl-4-carboxyphenylglycine (MCPG, *traces g* and *h*) was added during glutamate stimulation (open bars). In *trace i*, Ca^{2+} was removed from the bathing buffer. Experiments were repeated 34–48 times with similar results; one representative example is shown. *B*: effects of glutamate (100 μM; open bar) or ATP (100 μM; solid bar) on the $[Ca^{2+}]_i$ in non-neuronal cells present in the same cultures. Experiment was repeated 16 times with similar results.

Table 1. *Effects of Mg^{2+} or glycine on the glutamate- or NMDA-induced $[Ca^{2+}]_i$ increase in cerebellar granule cells*

	$[Ca^{2+}]_i$ Increase, % of Maximal Response	
Bathing Buffer	Glutamate	NMDA
$-Mg^{2+}$, +glycine	100	100
$-Mg^{2+}$, −glycine	82±9	1±0.1
$+Mg^{2+}$, +glycine	46±5	11±1
$+Mg^{2+}$, −glycine	15±2	2±0.1

Values are means ± SE for 16 independent experiments using different batches of cells. Effects of 100 μM glutamate or *N*-methyl-D-aspartate (NMDA) on cytosolic Ca^{2+} concentration ($[Ca^{2+}]_i$) was measured in the presence or absence of 1 mM Mg^{2+} and/or 10 μM glycine. Maximal response was seen in the presence of 10 μM glycine and absence of Mg^{2+}: 955±104 (n = 39) and 895±78 nM (n = 28) caused by glutamate and NMDA, respectively. Results are expressed as a percentage of the maximal response.

30 min at room temperature in 500 μl of lysis buffer that consisted of 10 mM Tris·HCl, 10 mM NaH_2PO_4/Na_2HPO_4, 130 mM NaCl, 1% Triton X-100, and 10 mM sodium pyrophosphate, pH 7.4. Aliquots of lysates (50 μl) were mixed with 10 μl of DEVD-AMC (1 μg/μl), which is the fluorogenic substrate for caspase-3, and 1 ml of 20 mM HEPES, 10% glycerol, and 2 mM dithiothreitol, pH 7.5, incubated for 60 min at 37°C. The fluorescence of the liberated product was measured using a spectrofluorometer (Spex Industries). The emission fluorescence spectrum was scanned between 400 and 480 nm using an excitation wavelength of 380 nm; active caspase-3 results in considerable emission at 440 nm. Caspase-3 activity was expressed as fluorescence intensity (in arbitrary units) in control and glutamate-treated cells. Experiments were repeated six times using different batches of cells, and similar results were observed. Capsase-1 and -8 activities were measured similarly using fluorometric assay kits according to the manufacturer's instructions. The means ± SE values for the fluorescence peak changes were calculated for n experiments.

Immunocytochemistry

Cells were plated in an eight-well chamber in the indicated concentrations of cytosine arabinoside for 7 days. After cells were washed twice in PBS, they were fixed in 4% paraformaldehyde for 10 min, rinsed twice in PBS, and permeabilized in 0.1% Triton X-100 for 10 min. After fixation, cells were incubated for 1 h with primary antibody (anti-glial fibrillary acidic protein), rinsed several times, and incubated for 1 h with goat anti-rabbit FITC-conjugated secondary antibody. Fluorescent cells were viewed using a standard fluorescence microscope (Axiophot; Zeiss, Jena, Germany). Experiments were repeated six times using different batches of cells with similar results. The results of one representative experiment are illustrated.

RESULTS

The cultures used in the present study contained both granule cells and glial cells. Although the growth of glial cells was minimized using the antimitotic cytosine arabinoside (10 μM), ~7% of the population was glial cells, which were identified by positive immunocytochemical staining for glial fibrillary acidic protein (see below) and their distinct morphology. After glutamate stimulation, the $[Ca^{2+}]_i$ of granule cells increased rapidly, whereas that of glial cells remained unchanged. Figure 1*A* shows results for granule cells in the presence of 10 μM glycine and the absence of Mg^{2+}, and, unless stated otherwise, in the presence of Ca^{2+}. Glutamate (100 μM) induced a rapid increase in $[Ca^{2+}]_i$ from a basal level of 44 ± 17 (n = 39) to 955 ± 104 nM (n = 39), and the $[Ca^{2+}]_i$ remained at this level as long as glutamate was present (*trace a*). Furthermore, reproducible $[Ca^{2+}]_i$ increases were evoked by repetitive stimulation with glutamate (*trace b*). The effect was predominantly due to activation of NMDA receptors, because it was completely abolished in the presence of MK-801 (*traces c* and *d*) but was unaffected by CNQX or MCPG, which are, respectively, non-NMDA ionotropic and metabotropic glutamate-receptor blockers (*traces e-h*). The inhibitory effect of MK-801 was irreversible in that glutamate was unable to induce a $[Ca^{2+}]_i$ increase after MK-801 washout (*trace d*). The glutamate-induced $[Ca^{2+}]_i$ increase was abolished in the absence of extracellular Ca^{2+}, which suggests that glutamate caused a Ca^{2+} influx (*trace i*). Glutamate did not cause an increase in the $[Ca^{2+}]_i$ in glial cells (Fig. 1*B*), whereas ATP (100 μM) did cause an increase in the $[Ca^{2+}]_i$ in glial cells (Fig. 1*B*) but not in granule cells (Fig. 1*A*, *trace j*).

We next measured the effects of Mg^{2+} and glycine on NMDA-receptor activation. As shown in Table 1, the maximal

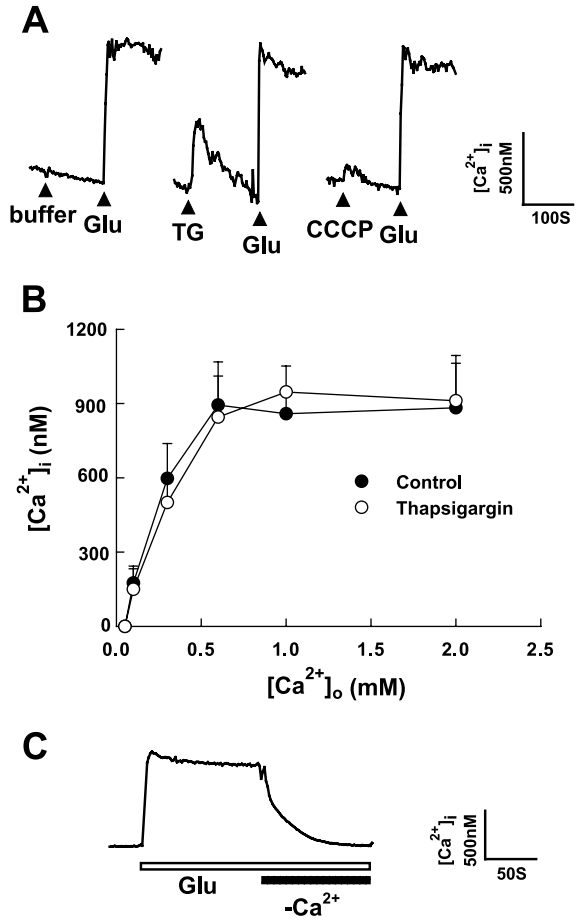

Fig. 2. Contribution of intracellular organelles to glutamate-induced $[Ca^{2+}]_i$ increase. *A*: 2 min after the cells were treated with buffer, 1 μM thapsigargin (TG), or 1 μM carbonyl cyanide *p*-trichloromethoxyphenylhydrazone (CCCP), 100 μM glutamate-induced $[Ca^{2+}]_i$ increase was measured. Experiments were repeated 14 times with similar results; one representative example is shown. *B*: cells were treated with buffer (control) or 1 μM thapsigargin for 3 min before $[Ca^{2+}]_i$ change was measured. Data shown are the changes in $[Ca^{2+}]_i$ induced by 100 μM glutamate in the presence of various concentrations of extracellular Ca^{2+} ($[Ca^{2+}]_o$). Results shown are means ± SE from four independent experiments using different batches of cells. *C*: after 2-min exposure to 100 μM glutamate, the $[Ca^{2+}]_i$ decreased to the basal level when extracellular Ca^{2+} was removed. Similar results were seen using four different batches of cells (n = 14).

glutamate-induced $[Ca^{2+}]_i$ increase was seen when cells were stimulated in the absence of Mg^{2+} and the presence of 10 μM glycine, which is a typical phenomenon of NMDA-receptor activation (35). In the absence of glycine or the presence of Mg^{2+}, the magnitude of the glutamate-induced $[Ca^{2+}]_i$ increase was reduced. The respective $[Ca^{2+}]_i$ increases were 82 ± 9 (n = 28) or 46 ± 5% (n = 28) of the maximal responses, whereas in the combined absence of glycine and presence of Mg^{2+}, the magnitude of the $[Ca^{2+}]_i$ increase was further reduced to 15 ± 2% (n = 28) of the maximal response. A similar inhibitory effect of Mg^{2+} and stimulatory effect of glycine on the $[Ca^{2+}]_i$ increase was seen when the cells were stimulated with 100 μM NMDA (Table 1), except that the response was completely abolished in the absence of glycine in both the presence and absence of Mg^{2+}. Unless otherwise stated, the experiments described below on control and glutamate-stimulated cells were performed in the absence of Mg^{2+} and the presence of 10 μM glycine to observe the maximal response of NMDA-receptor activation.

Taken together, our data suggest that in cerebellar granule cells, glutamate-induced $[Ca^{2+}]_i$ increase is mainly mediated by the Ca^{2+} influx via the activation of NMDA receptors (Fig. 1 and Table 1). To further characterize the contribution of intracellular Ca^{2+} release to glutamate-induced $[Ca^{2+}]_i$ increase, three different experiments were undertaken. First, we compared glutamate-induced $[Ca^{2+}]_i$ increases in cells with or without the prior treatment of thapsigargin or CCCP. Thapsigargin, a sarco(endo)plasmic reticulum Ca^{2+} ATPase inhibitor, depletes intracellular nonmitochondrial Ca^{2+} stores, whereas CCCP, a proton ionophore, prevents Ca^{2+} loading within mitochondria. As shown in Fig. 2*A*, thapsigargin (1 μM) and CCCP (1 μM) both induced a slight but slow $[Ca^{2+}]_i$ increase in granule cells. The subsequent response of the $[Ca^{2+}]_i$ increase evoked by glutamate in both cases remained indistinguishable from that of control cells; the glutamate-induced $[Ca^{2+}]_i$ changes were 934 ± 88, 902 ± 103, and 965 ± 114 nM (n = 14), in control, thapsigargin-, and CCCP-pretreated cells, respectively. Second, it is possible that the Ca^{2+} influx via NMDA receptors is the trigger to induce Ca^{2+} release from intracellular Ca^{2+} stores (the so-called Ca^{2+}-induced Ca^{2+}-release mechanism). Then, the higher the extracellular Ca^{2+} concentration, the more Ca^{2+} enters cells via NMDA receptors, and the greater the final $[Ca^{2+}]_i$ increase is seen in cells in response to the stimulation of glutamate. If this were the case, the EC_{50} values for extracellular Ca^{2+} in glutamate-induced $[Ca^{2+}]_i$ increases would be changed after intracellular Ca^{2+} stores were depleted by thapsigargin. As shown in Fig. 2*B*, glutamate-induced $[Ca^{2+}]_i$ increases were measured in various extracellular Ca^{2+} concentrations in both control and thapsigargin-treated cells. The EC_{50} values for the extracellular Ca^{2+} concentrations, 0.25 and 0.26 mM, respectively, were not significantly different in these two cases. Finally, we measured the decline of increased $[Ca^{2+}]_i$ induced by glutamate in response to the removal of extracellular Ca^{2+} while glutamate was still present. The $[Ca^{2+}]_i$ would not return to the basal level if intracellular Ca^{2+} release contributed the Ca^{2+} signal. In fact, as shown in Fig. 2*C*, the increased $[Ca^{2+}]_i$ returned to the basal level rapidly after extracellular Ca^{2+} was removed.

In granule cells, glutamate produced a dose-dependent increase in $[Ca^{2+}]_i$ (Fig. 3*A*); the maximal effect was seen at 100 μM glutamate, and the EC_{50} value was 12 μM. Glutamate treatment also resulted in cytotoxicity. To avoid interference from the protective effect of neurotrophins present in serum, in preliminary experiments the cells were exposed to glutamate and then incubated in serum-free medium (DMEM) for different periods of time before LDH release was measured. After 4 h at 37°C in serum-free medium, considerable cell death was seen in glutamate-treated cells while basal cell death was low. Unless stated otherwise, the cell death experiments described below were performed after a 4-h incubation in serum-free medium following glutamate treatment. Using Trypan blue exclusion, 7% of the cells scraped off dishes without any treatment whatsoever were found to be dead, and this percentage increased to 15% for cells incubated first for 30 min in glycine that contained Mg^{2+}-free buffer and then for 4 h at

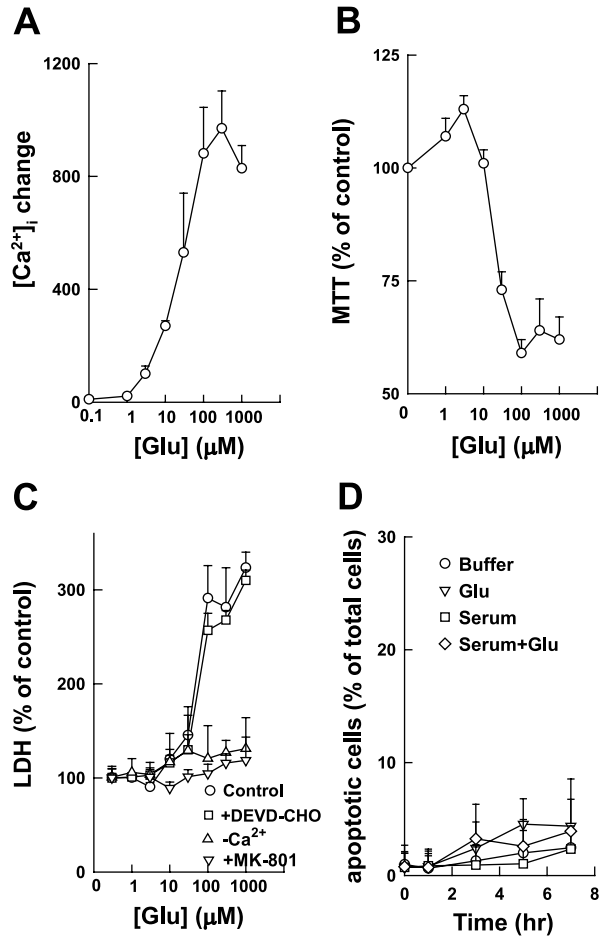

Fig. 3. Concentration and time dependence of the effect of glutamate on $[Ca^{2+}]_i$ and cell death in cerebellar granule cells. *A*: $[Ca^{2+}]_i$ increase. Data are means ± SE for 32 experiments from different batches of cells. *B*, *C*, *D*: glutamate-induced cell death expressed as decrease in 3-(4,5-dimethylthiazol-2-yl)-2,5-diphenyltetrazolium bromide (MTT) reduction, increase in lactate dehydrogenase (LDH) release, or increase in the percentage of apoptotic cells, respectively. Glutamate-induced LDH release was also measured in the absence of Ca^{2+} or the presence of 10 μM MK-801 or 10 μM DEVD-CHO. Results in *B* and *C* are expressed as a percentage of the control value for cells incubated in the same glycine-containing Mg^{2+}-free buffer in the absence of glutamate and then incubated for 4 h at 37°C in serum-free medium in the same way as glutamate-treated cells. Number of apoptotic cells induced by glutamate was also measured in the presence of 10% serum after glutamate exposure and the results are expressed as the percentage of the total cells. Data are means ± SE for six independent experiments using different batches of cells.

37°C in serum-free medium before detachment from the culture dishes. Thus the basal cell death (control) caused by incubating cells in glycine-containing Mg^{2+}-free buffer for 30 min and then in serum-free medium at 37°C for 4 h was ~8% (data not shown). As shown in Fig. 3*B*, MTT reduction by succinate dehydrogenase in living cells was reduced following the 30-min exposure of cells to glutamate concentrations >10 μM while LDH release increased (Fig. 3C). Both effects were saturable, and the degree of cytotoxicity was dependent on the glutamate concentration. The EC_{50} values for glutamate were 25 and 38 μM in the MTT reduction and LDH release assays, respectively; the maximal effect was seen with 100 μM glutamate in both assays. To examine the role of Ca^{2+} in the cytotoxic effects of glutamate, we measured glutamate-induced LDH release in the absence of extracellular Ca^{2+} and found that removal of extracellular Ca^{2+} completely protected the cells from glutamate-induced cytotoxicity (Fig. 3*C*). The NMDA-receptor inhibitor MK-801 also blocked glutamate-induced cytotoxicity, whereas the caspase-3 inhibitor DEVD-CHO had no effect (Fig. 3*C*). When the chromatin-specific dye Hoechst 33258 was used to measure apoptotic and nonapoptotic bodies in cells exposed to glutamate for 30 min and then incubated in the presence and absence of serum for ≤7 h, no difference in the percentage of apoptotic cells was seen in control and glutamate-treated cells and in cells incubated in the presence or absence of serum (Fig. 3*D*). This suggests that glutamate-induced apoptosis was negligible within 7 h.

To elucidate the biochemical basis for the cytotoxic effect of glutamate and the potential protective mechanisms, we tested the effects of GSNO on glutamate-induced cytotoxicity, which was measured using LDH release. As shown in Fig. 4*A*, glutamate-induced LDH release was reduced by ~75% in the presence of 1 mM GSNO. NO is readily released from GSNO to form GSH. To further characterize the cytoprotective mechanism of GSNO, we examined the effects of SNAP (another NO donor) and GSH on glutamate-induced cytotoxicity. As shown in Fig. 4*A*, the presence of 1 mM GSH during the 30-min glutamate stimulation period did not affect glutamate-induced LDH release, whereas 1 mM SNAP had a similar protective effect to that seen with GSNO. Figure 4*B* shows that

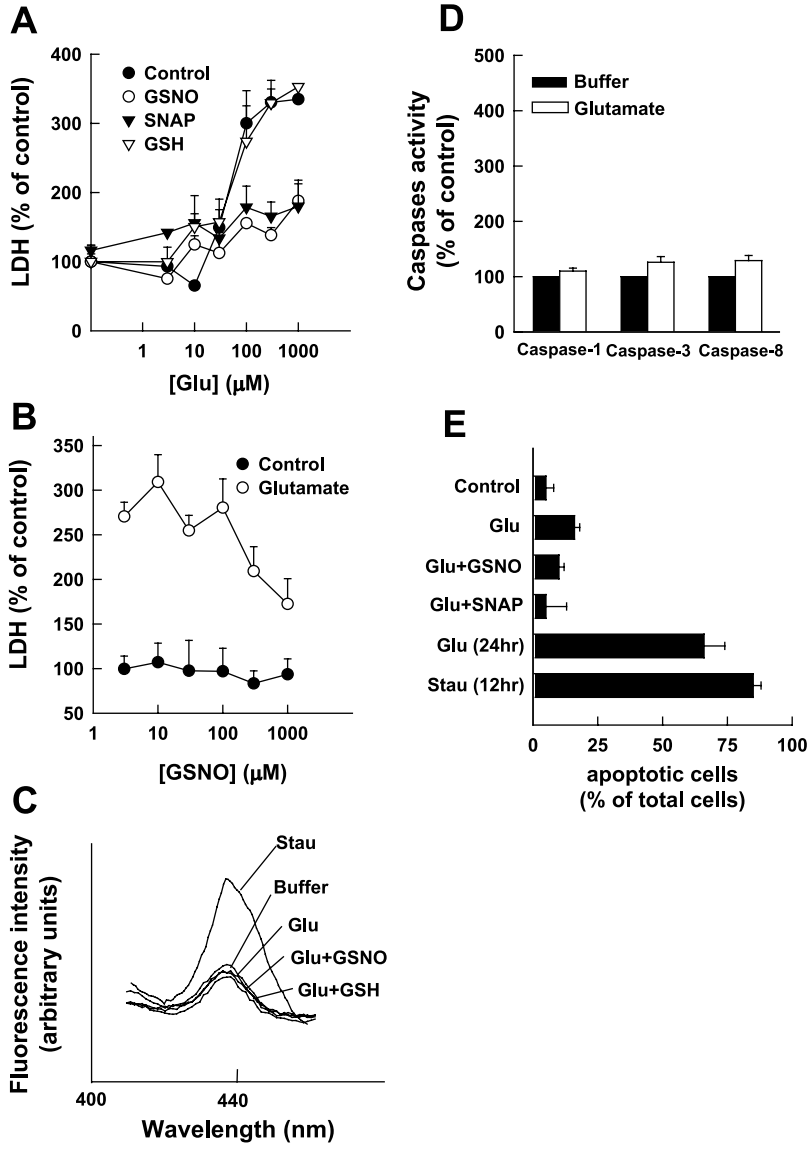

Fig. 4. Effects of *S*-nitrosoglutathione (GSNO) or *S*-nitroso-*N*-acetylpenicillamine (SNAP) on glutamate-induced cytotoxicity. Buffer used contained 10 μM glycine and was Mg^{2+} free. *A*: concentration dependence of the effects of glutamate on LDH release in the absence or presence of 1 mM GSNO, 1 mM SNAP, or 1 mM glutathione (GSH). Results are means ± SE for five independent experiments. *B*: basal (buffer only; control) and 100 μM glutamate-induced LDH release measured at various concentrations of GSNO. Data are means ± SE for five independent experiments. *C*: effects of glutamate on caspase-3 activation. Emission fluorescence spectra (400–480 nm) of the cleavage product of caspase-3 following treatment of cells with buffer, 100 μM glutamate alone, or 100 μM glutamate plus either 1 mM GSNO or 1 mM GSH for 30 min and incubation for 4 h at 37°C in serum-free medium or 0.3 μM staurosporine (Stau) for 12 h. Experiments were repeated six times with similar results; one representative trace is shown. *D*: statistical data for caspase activity induced by buffer or glutamate. Activities of different caspases induced by glutamate were calculated from means ± SE values for the fluorescence peak changes (n = 6–8) and are expressed as percentages of the control value in the presence of buffer. *E*: number of apoptotic cells was measured 4 h after treatment of cells with buffer (control), 100 μM glutamate alone, or 100 μM glutamate plus either 1 mM GSNO or 1 mM SNAP for 30 min. Number of apoptotic cells was also measured 24 h after cells were treated with 100 μM glutamate for 30 min [Glu (24 h)] or after cells were treated with 0.3 μM staurosporine for 12 h [Stau (12 h)]. Results expressed as percentages of total cells. Data are means ± SE for six independent experiments using different batches of cells.

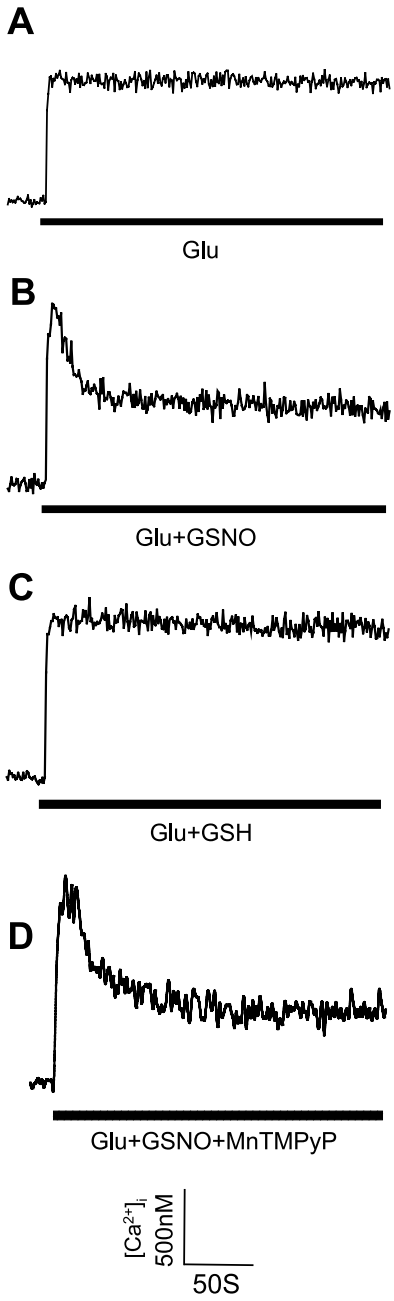

Fig. 5. Effects of GSNO or GSH on the glutamate-induced $[Ca^{2+}]_i$ increase. Change in $[Ca^{2+}]_i$ induced by 100 μM glutamate was measured in the absence (*A*) or presence (*B*) of 1 mM GSNO, 1 mM GSH (*C*), or 1 mM GSNO plus 5 μM manganese (III) tetrakis(1-methyl-4-pyridyl)porphyrin (MnTMPyP; *D*). Experiments were repeated 18–24 times using six different batches of cells, and similar results were seen; one representative example is shown.

GSNO had a concentration-dependent protective effect on glutamate-induced cytotoxicity and that GSNO itself had no direct effect on LDH release.

Activation of caspases leads to cell death. We therefore determined whether caspases were activated by glutamate in the presence or absence of GSNO and GSH. As shown in Fig. 4*C*, caspase-3 activity was unaffected by any of these treatments. For a positive control, we measured the caspase-3 activity after treatment of cells for 12 h with the protein kinase C inhibitor staurosporine and found that this treatment results in increased caspase-3 activity (Fig. 4*C*). We also measured caspase-1 and -8 activities after glutamate stimulation and found that neither was increased. The statistical data for the activities of all three caspases before and after glutamate stimulation are summarized in Fig. 4*D*. Consistent with the caspase activities, no significant apoptotic cells were found 4 h after glutamate treatment regardless of the presence of GSNO or SNAP, whereas apoptotic cells increased to 66 ± 8% after 24 h (Fig. 4*E*). A similar quantity of apoptotic cells was seen after cells were treated with staurosporine for 12 h.

As shown in Fig. 5, coexposure of cells to glutamate and GSNO resulted in a transient peak in the $[Ca^{2+}]_i$ followed by a decrease to a lower plateau level (a "transient" response) instead of the "sustained" increase seen with glutamate alone (Fig. 5, compare *B* and *A*), whereas coexposure to glutamate and GSH yielded a response indistinguishable from that with glutamate alone (Fig. 5*C*); in all cases, the peak $[Ca^{2+}]_i$ increase was the same. The transient $[Ca^{2+}]_i$ increase seen when cells were exposed to glutamate and GSNO was unaffected by the presence of MnTMPyP (Fig. 5*D*), which scavenges the ROS generated (16).

As shown in Fig. 6, GSNO did not affect the action of thapsigargin or CCCP on $[Ca^{2+}]_i$ increase. It only modified the

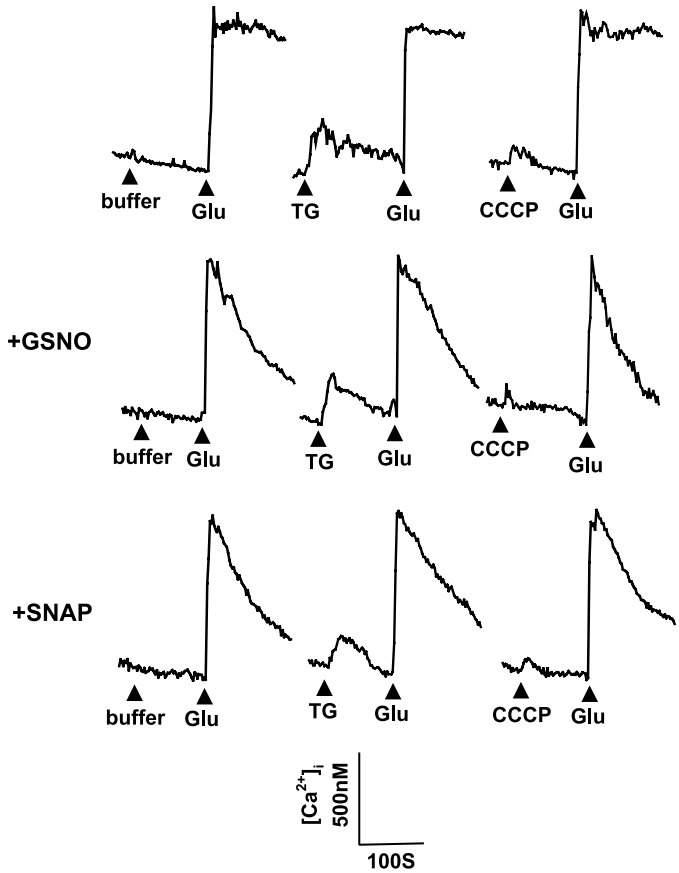

Fig. 6. Lack of effect of nitric oxide (NO) on thapsigargin- and CCCP-induced $[Ca^{2+}]_i$ increase. Changes in $[Ca^{2+}]_i$ shown were measured in the absence (*top*) or presence (*middle*) of 1 mM GSNO or 1 mM SNAP (*bottom*). Cells were initially exposed to buffer, 1 μM thapsigargin, or 1 μM CCCP as indicated (arrowheads). Glutamate (100 μM) was then added in all cases. Experiments were repeated 12 times using different batches of cells, and similar results were seen; one representative example is shown.

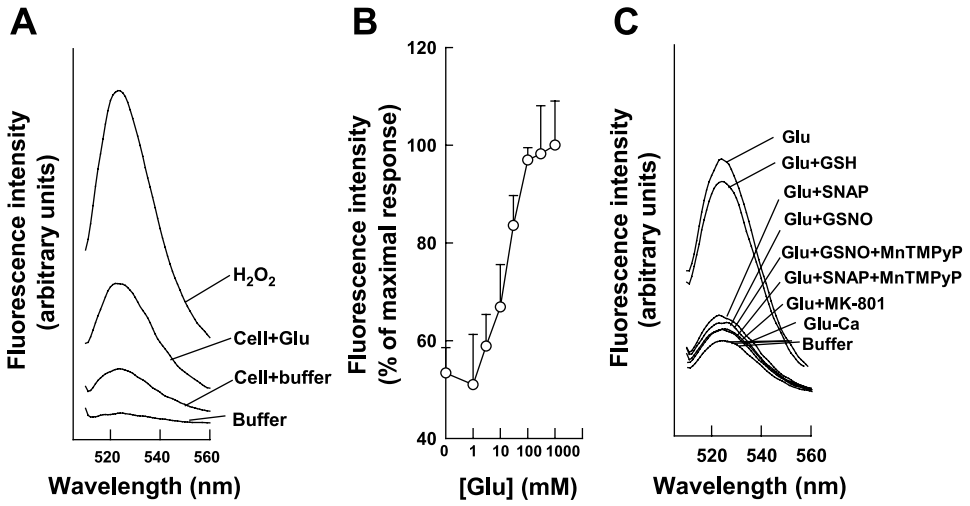

Fig. 7. Effects of GSNO, SNAP, or GSH on glutamate-induced reactive oxygen species (ROS) generation. *A*: emission spectra (500–560 nm) of the fluorogenic product dichlorodihydrofluorescein (DCF) produced by incubation with H_2O_2 or buffer, or intracellular ROS in cells treated with buffer or 100 μM glutamate. *B*: concentration dependence of the effects of glutamate on ROS generation. Fluorescence intensity at 525 nm was plotted vs. the glutamate concentration. Amount of ROS generation is expressed as a percentage of that induced by 1,000 μM glutamate. Data are means ± SE for eight independent experiments. *C*: ability of ROS within cells to oxidize the fluorogenic dye after incubation of cells with buffer or 100 μM glutamate in the absence of Ca^{2+} (Glu-Ca) or in presence of Ca^{2+} plus 10 μM MK-801, 1 mM GSNO, 1 mM GSH, 1 mM SNAP, 1 mM GSNO and 5 μM MnTMPyP, or 1 mM SNAP and 5 μM MnTMPyP. Experiment was repeated nine times with similar results; one representative example is shown.

glutamate-induced $[Ca^{2+}]_i$ change by switching sustained increase to transient response, even though glutamate stimulation was undertaken after intracellular Ca^{2+} stores were depleted by thapsigargin or CCCP (compare Fig. 6 with Fig. 2*A*). SNAP displayed a similar effect as GSNO on $[Ca^{2+}]_i$ increases induced by glutamate after cells were treated with buffer, thapsigargin, or CCCP.

Generation of excess ROS within cells can cause cytotoxicity. We therefore examined whether glutamate induced the generation of ROS in granule cells and if so, whether this was affected by GSNO and GSH. In the absence of the fluorogenic dye H_2DCFDA, no fluorescence was seen in the presence of buffer, H_2O_2, or untreated or glutamate-treated cells (data not shown). As shown in Fig. 7*A*, in the presence of the dye, buffer did not cause significant fluorescence emission. Although 100 μM H_2O_2 oxidized the dye and generated a fluorescent product, control cells caused a small but significant amount of ROS to be generated, while glutamate-stimulated cells yielded a marked increase in fluorescence. Figure 7*B* summarizes the dependence of ROS generation in granule cells on the glutamate concentration. The maximal response was seen at 100 μM glutamate and the EC_{50} was 22 μM. As shown in Fig. 7*C*, the glutamate-induced generation of ROS was not significantly affected by simultaneous treatment of the cells with GSH (1

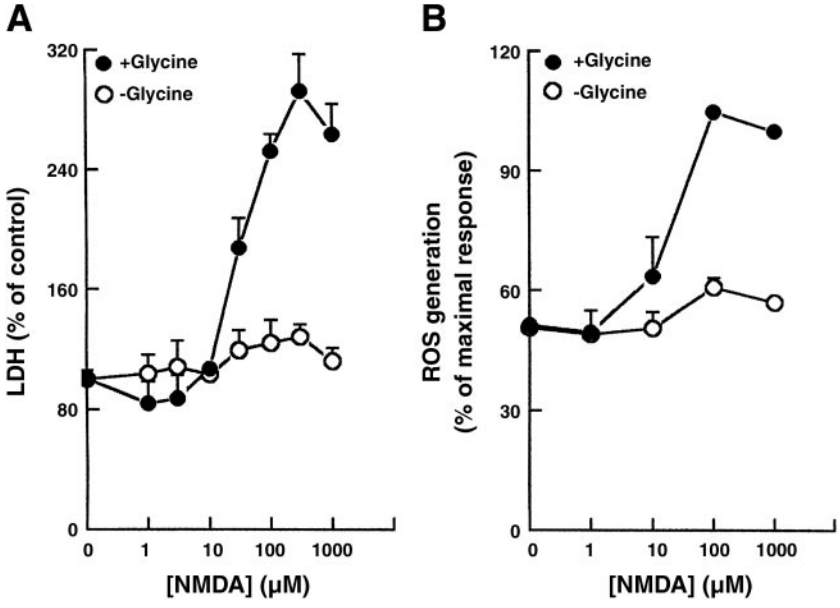

Fig. 8. Concentration dependence of the effects of NMDA on LDH release and ROS generation. *A*: LDH release in response to various concentrations of NMDA in the absence of Mg^{2+} and the presence or absence of 10 μM glycine. Results are expressed as a percentage of control values without NMDA stimulation. *B*: ROS generation in response to various concentrations of NMDA in the absence of Mg^{2+} and the presence or absence of 10 μM glycine. ROS generation is expressed as a percentage of that induced by 1,000 μM NMDA. Data are means ± SE for six independent experiments using different batches of cells.

mM), whereas 1 mM GSNO or SNAP completely blocked the effect regardless of the presence of MnTMPyP as did removal of extracellular Ca^{2+} or inhibition of the NMDA receptor by MK-801. Figure 8 shows that stimulation of cells with NMDA also resulted in ROS generation and cell death, and that both were dependent on the concentration of NMDA with the maximal effect seen at 100 μM; even in the absence of Mg^{2+}, these effects were not observed in the absence of glycine.

Our results show that in granule cells, a $[Ca^{2+}]_i$ increase, ROS generation, and cytotoxicity were all induced by glutamate, and that all three effects were blocked by removal of extracellular Ca^{2+}. We next determined whether the sustained $[Ca^{2+}]_i$ increase induced by glutamate led to the generation of ROS, which subsequently caused cell death, by testing the effects of glutamate on $[Ca^{2+}]_i$ increase and cell death in the presence of MnTMPyP. As shown in Fig. 9*A*, MnTMPyP had no effect on the glutamate-induced $[Ca^{2+}]_i$ increase but did abolish glutamate-induced cytotoxicity (Fig. 9*B*).

Neurotrophins produced by glial cells are neuroprotective. Because the cultures used in this study contained both neuronal and non-neuronal cells, we determined whether increasing the percentage of glial cells in the cultures by reducing the cytosine arabinoside concentration in the medium from 10 to 5 μM or zero protected granule cells against glutamate-induced cytotoxicity. As shown in Fig. 10, glutamate-induced cytotoxicity, measured either by LDH release (Fig. 10*B*) or MTT reduction assay (Fig. 10*C*), was unaffected, although the content of glial cells was significantly different among three cultures (Fig. 10*A*).

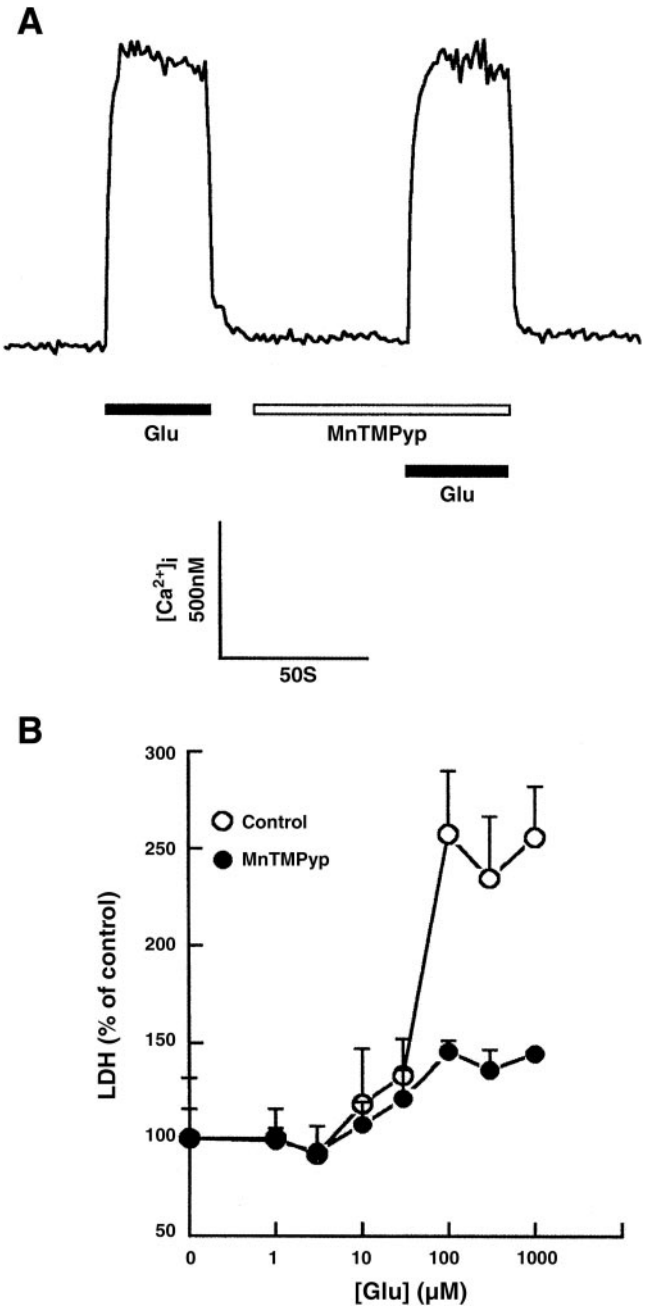

Fig. 9. Effects of an ROS scavenger on the glutamate-induced $[Ca^{2+}]_i$ increase and cell death. *A*: glutamate (100 μM) induced a $[Ca^{2+}]_i$ increase before and after treatment of cells with 5 μM MnTMPyP for 1 min as indicated by horizontal bars. Experiment was repeated 12 times with similar results. *B*: glutamate-induced LDH release at the indicated glutamate concentration measured after exposure of cells to medium or 5 μM MnTMPyP for 30 min. Results are expressed as a percentage of control values without glutamate stimulation. Data are means ± SE for six independent experiments using different batches of cells.

DISCUSSION

In the present study, we found that in granule cells, the glutamate-evoked $[Ca^{2+}]_i$ increase, as measured using the indicator fura-2, was predominantly due to activation of NMDA receptors since it was not inhibited by CNQX or MCPG but was completely inhibited by MK-801 and was dependent on extracellular Ca^{2+} (see Fig. 1). The inhibitory effect of Mg^{2+} and the stimulatory effect of glycine on the glutamate-induced $[Ca^{2+}]_i$ increase is further evidence for involvement of the NMDA receptor (see Table 1). Glutamate also induced ROS generation and cell death, and both events were dependent on glutamate-induced Ca^{2+} influx and were inhibited by MK-801 (see Figs. 3 and 7). Thus in granule cells, activation of the NMDA receptor leads to a $[Ca^{2+}]_i$ increase, ROS generation, and cell death. Similar results were seen using NMDA (see Table 1 and Fig. 8). Furthermore, the EC_{50} values for glutamate for the $[Ca^{2+}]_i$ increase, ROS generation, and cell death were consistent at 12, 22, and 25 μM, respectively (see Figs. 3, 4, and 7).

In the absence of extracellular Ca^{2+} or the presence of an intracellular Ca^{2+} chelator, neurons survive after NMDA-receptor stimulation (8, 43), which indicates that Ca^{2+} influx through the NMDA receptor may be the primary event triggering glutamate-induced neuronal injury. In the present study, we observed that the $[Ca^{2+}]_i$ increase that resulted from activation of NMDA receptors was sustained while glutamate was present, and that reproducible $[Ca^{2+}]_i$ increases were seen following repetitive glutamate stimulation, which suggests that inactivation and desensitization of the NMDA receptor did not occur as long as glutamate was present (see Fig. 1). We also demonstrated a direct connection between the sustained glutamate-induced $[Ca^{2+}]_i$ increase and ROS generation. When the sustained $[Ca^{2+}]_i$ increase was inhibited by GSNO, despite a transient $[Ca^{2+}]_i$ increase, ROS generation was abolished and cell injury did not occur (see Figs. 4, 5, and 7). Thus in granule cells, glutamate-induced ROS generation is dependent on a

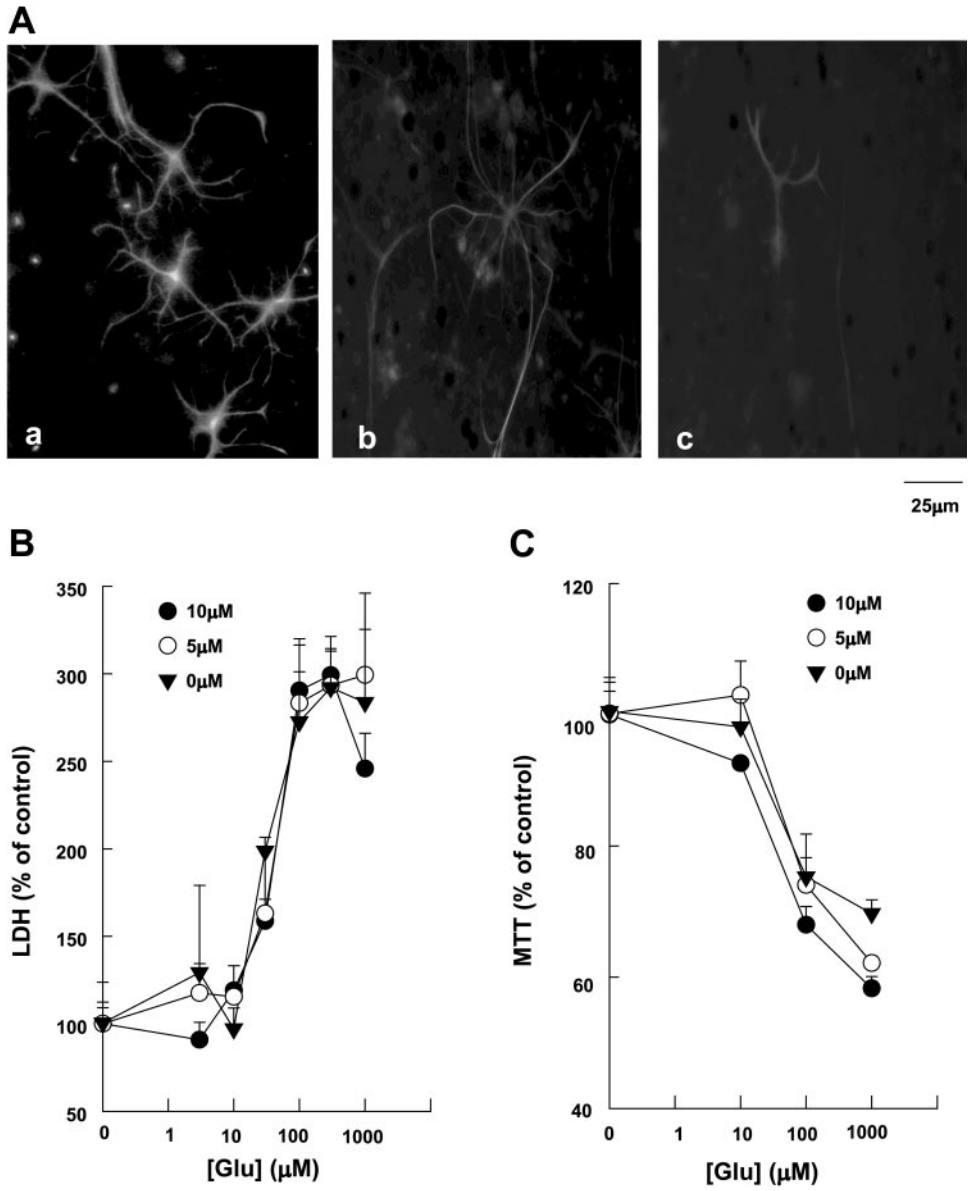

Fig. 10. Lack of effect of the number of glial cells in the culture on glutamate-induced cell death. *A*: cultures were grown in medium containing 0 (*a*), 5 (*b*), or 10 μM (*c*) cytosine arabinoside. Glial cells, which were present in the cultures used, were immunocytochemically identified by glial fibrillary acidic protein as described in MATERIALS AND METHODS. Experiments were repeated six times using different batches of cells. One representative sample is shown. *B*: LDH assay. *C*: MTT reduction. Cell death caused by the indicated glutamate concentrations in different cultures as described in *A* was determined via the methods in *B* and *C*. Data are means ± SE for five independent experiments using different batches of cells.

sustained $[Ca^{2+}]_i$ increase that leads to cell death; a transient $[Ca^{2+}]_i$ increase is not sufficient to produce these effects.

Our results also demonstrated the temporal sequence of the actions of these cellular mediators that are generated following glutamate stimulation and lead to cell death. Scavenging of ROS protected cells against glutamate-induced cytotoxicity but had no effect on the glutamate-induced $[Ca^{2+}]_i$ increase; this suggests that the increase in the $[Ca^{2+}]_i$ precedes ROS generation, which then leads to cell death (see Fig. 9). Many studies have shown that the massive influx of Ca^{2+} that results from NMDA-receptor activation is taken up not only by the endoplasmic reticulum but also by mitochondria (22, 39, 44, 45). Excessive Ca^{2+} sequestration into mitochondria can result in mitochondrial dysfunction, which includes impaired ATP production, generation of ROS, and the opening of the permeability transition pore, and finally leads to cell death (4, 23, 36). The mitochondrion might therefore be the critical organelle linking glutamate-induced Ca^{2+} influx and cell injury. In the present study, our results suggest that in granule cells, the contribution of Ca^{2+} release from intracellular Ca^{2+} stores to glutamate-induced $[Ca^{2+}]_i$ increase is negligible (see Fig. 2). The transient $[Ca^{2+}]_i$ increase caused by glutamate in the presence of GSNO still seen after the actions of thapsigargin or CCCP (see Fig. 6) suggest that the transient $[Ca^{2+}]_i$ increase was probably due to inactivation of NMDA receptors rather than an excessive Ca^{2+} sequestration into intracellular organelles. Because changes in the $[Ca^{2+}]_i$ reflect the final $[Ca^{2+}]_i$ after the operation of all Ca^{2+} transporters within the cell, it is possible that the activities of other Ca^{2+} transporters are modified by nitrosylation, nitration, or oxidation induced by an NO donor. For example, Ca^{2+} extrusion from the cell via the Ca^{2+} pump and Na^+/Ca^{2+} exchanger are accelerated, with the result that the $[Ca^{2+}]_i$ falls back to the basal level.

The culture medium used in this study contained serum, cytosine arabinoside, and a high K^+ concentration (final concentration, ~25 mM), which favor the growth of neurons.

Concurrently, granule cells undergo rapid biochemical and morphological differentiation (19, 29). Thus granule cells are enriched and make up the majority of cells in the cultures. Reducing the K^+ concentration in the medium promotes the degeneration of granule cells via caspase activation (14, 47), whereas reducing the cytosine arabinoside concentration increases the percentage of glial cells in the cultures. Many studies have shown caspase activation to be responsible for NMDA-induced neurotoxicity (42). In the current study in which cell cultures were grown in a high-K^+ medium, the activities of caspase-1, -3, and -8 were not increased 4 h following glutamate stimulation, inhibition of caspase-3 did not block glutamate-induced cytotoxicity, and apoptotic cell death was not seen until 24 h after exposure of cells to glutamate (see Figs. 3 and 4). Furthermore, increasing the percentage of glial cells in the cultures by reducing the cytosine arabinoside concentration did not prevent glutamate-induced excitotoxic injury (Fig. 10). Because the cultures used contained a mixture of cells, it is possible that the cell death detected involved predominantly glial cells rather than granule cells, in which case increasing the number of glial cells would not be expected to result in protection of granule cells. However, this is unlikely, because glial cells did not respond to glutamate stimulation (see Fig. 1).

Glycine is the coagonist for NMDA-receptor activation. The maximal effect of NMDA-receptor activation on $[Ca^{2+}]_i$ increase, ROS generation, and cell death was seen in the presence of glycine and the absence of Mg^{2+} (see Table 1 and Fig. 8). Glycine was absolutely required for the action of NMDA; in its absence, NMDA did not induce any measurable increase in $[Ca^{2+}]_i$ even in the absence of Mg^{2+} (see Table 1), and ROS generation and cell death were not observed (see Fig. 8). This is further evidence for the above-mentioned dependence of NMDA-receptor activation-induced ROS generation and cell death on the $[Ca^{2+}]_i$ increase. In terms of the action of glutamate on the $[Ca^{2+}]_i$ increase, removal of Mg^{2+} had a greater effect than the presence of glycine (see Table 1).

GSH acts as an NMDA-receptor agonist in the central nervous system (28, 38). In the present study, in the presence of glycine and absence of Mg^{2+}, neither GSH nor GSNO alone was able to induce a $[Ca^{2+}]_i$ increase via the NMDA receptor (data not shown), and GSNO alone could not induce cell death (see Fig. 4), which indicates that in granule cells, GSH is not an NMDA-receptor agonist. However, the sustained glutamate-induced $[Ca^{2+}]_i$ increase was replaced by a transient $[Ca^{2+}]_i$ increase in the presence of GSNO. Our results also show that it was the NO component rather than the GSH component of GSNO that modulated the effect of glutamate on NMDA-receptor activation, since another NO donor, SNAP, mimicked the effect of GSNO on $[Ca^{2+}]_i$ increase, ROS generation, and cell death, whereas GSH did not (see Figs. 4, 5, and 7). Granule cells are NO-producing neurons (25). Using immunoblotting, we measured nitric oxide synthase (NOS)-1 expression in cells exposed to glutamate for 30 min in the presence or absence of serum and then left for 4 h in serum-free medium. Granule cells were found to express significant amounts of NOS-1, but this was unaffected by glutamate treatment in the presence or absence of serum (data not shown). Our result showing the high vulnerability of granule cells to exogenously added NO suggests that under our defined experimental conditions, endogenously generated NO was not produced in large enough amounts to modify the NMDA receptor. One possibility was that the free radicals generated in the presence of glutamate might interact with the NO produced by GSNO to generate peroxynitrite, which might be responsible for the modified NMDA-receptor channel activity. However, the fact that a transient $[Ca^{2+}]_i$ increase and the abolishment of ROS generation were still seen when a free-radical scavenger was coapplied with the glutamate and GSNO indicates that the amount of peroxynitrite formed was negligible (see Figs. 5*D* and 7) and so did not affect NMDA-channel activity.

In conclusion, in rat cerebellar granule neurons, activation of the NMDA receptor results in a sustained $[Ca^{2+}]_i$ increase, ROS generation, and cell death, all of which are prevented by coexposure of the cells to GSNO.

ACKNOWLEDGMENTS

We thank Dr. Thomas Barkas for helpful discussion.

GRANTS

This work was supported by National Science Council Grant NSC91-2320-B016-015 and National Defense Medical Center, Republic of China Grant DOD-91-14.

REFERENCES

1. **Broillet MC and Firestein S.** Direct activation of the olfactory cyclic nucleotide-gated channel through modification of sulfhydryl groups by NO compounds. *Neuron* 16: 377–385, 1996.
2. **Broillet MC and Firestein S.** Beta subunits of the olfactory cyclic nucleotide-gated channel form a nitric oxide activated Ca^{2+} channel. *Neuron* 18: 951–958, 1997.
3. **Campbell DL, Stamler JS, and Strauss HC.** Redox modulation of L-type calcium channels in ferret ventricular myocytes. Dual mechanism regulation by nitric oxide and *S*-nitrosothiols. *J Gen Physiol* 108: 277–293, 1996.
4. **Castilho RF, Hansson O, Ward MW, Budd SL, and Nicholls DG.** Mitochondrial control of acute glutamate excitotoxicity in cultured cerebellar granule cells. *J Neurosci* 18: 10277–10286, 1998.
5. **Cathcart R, Schwiers E, and Ames BN.** Detection of picomole levels of hydroperoxides using a fluorescent dichlorofluorescein assay. *Anal Biochem* 134: 111–116, 1983.
6. **Cebers G, Cebere A, and Liljequist S.** Metabolic inhibition potentiates AMPA-induced Ca^{2+} fluxes and neurotoxicity in rat cerebellar granule cells. *Brain Res* 779: 194–204, 1998.
7. **Chin TY, Hwang HM, and Chueh SH.** Distinct effects of different calcium-mobilizing agents on cell death in NG108–15 neuroblastoma × glioma cells. *Mol Pharmacol* 61: 486–494, 2002.
8. **Choi DW.** Ionic dependence of glutamate neurotoxicity. *J Neurosci* 7: 369–379, 1987.
9. **Choi DW.** Glutamate neurotoxicity and diseases of the nervous system. *Neuron* 1: 623–634, 1988.
10. **Chueh SH, Song SL, and Liu TY.** Heterologous desensitization of opioid-stimulated Ca^{2+} increase by bradykinin or ATP in NG108–15 cells. *J Biol Chem* 270: 16630–16637, 1995.
11. **Coyle JT and Puttfarcken P.** Oxidative stress, glutamate, and neurodegenerative disorders. *Science* 262: 689–695, 1993.
12. **Cunningham AJ and Szenberg A.** Further improvements in the plaque technique for detecting single antibody-forming cells. *Immunology* 14: 599–601, 1968.
13. **Dawson VL, Dawson TM, London ED, Bredt DS, and Snyder SH.** Nitric oxide mediates glutamate neurotoxicity in primary cortical cultures. *Proc Natl Acad Sci USA* 88: 6368–6371, 1991.
14. **D'Mello SR, Aglieco F, Roberts MR, Borodezt K, and Haycock JW.** A DEVD-inhibited caspase other than CPP32 is involved in the commitment of cerebellar granule neurons to apoptosis induced by K^+ deprivation. *J Neurochem* 70: 1809–1818, 1998.
15. **Dugan LL, Sensi SL, Canzoniero LMT, Handran SD, Rothman SM, Lin TS, Goldberg MP, and Choi DW.** Mitochondrial production of

reactive oxygen species in cortical neurons following exposure to *N*-methyl-D-aspartate. *J Neurosci* 15: 6377–6388, 1995.
16. **Faulkner KM, Liochev SI, and Fridovich I.** Stable Mn(III) porphyrins mimic superoxide dismutase in vitro and substitute for it in vivo. *J Biol Chem* 269: 23471–23476, 1994.
17. **Frandsen A and Schousboe A.** Excitatory amino acid-mediated excitotoxicity and calcium homeostasis in cultured neurons. *J Neurochem* 60: 1202–1211, 1993.
18. **Gallo V, Ciotti MT, Coletti A, Aloisi F, and Livi G.** Selective release of glutamate from cerebellar granule cells differentiating in culture. *Proc Natl Acad Sci USA* 79: 7919–7923, 1982.
19. **Gallo V, Kingsbury A, Balazs R, and Jorgensen OS.** The role of depolarization in the survival and differentiation of cerebellar granule cells in culture. *J Neurosci* 7: 2203–2213, 1987.
20. **Grynkiewicz G, Poenie M, and Tsien RY.** A new generation of Ca^{2+} indicators with greatly improved fluorescence properties. *J Biol Chem* 260: 3440–3450, 1985.
21. **Johnson JW and Ascher P.** Glycine potentiates the NMDA response in cultured mouse brain neurons. *Nature* 325: 529–531, 1987.
22. **Khodorov B, Pinelis V, Storozhevykh T, Vergun O, and Vinskaya N.** Dominant role of mitochondria in protection against a delayed neuronal Ca^{2+} overload induced by endogenous excitatory amino acids following a glutamate pulse. *FEBS Lett* 393: 135–138, 1996.
23. **Khodorov B, Pinelis V, Storozhevykh T, Yuravichus A, and Khaspekhov L.** Blockade of mitochondrial Ca^{2+} uptake by mitochondrial inhibitors amplifies the glutamate-induced calcium response in cultured cerebellar granule cells. *FEBS Lett* 458: 162–166, 1999.
24. **Koh JY and Choi DW.** Quantitative determination of glutamate mediated cortical neuronal injury in cell culture by lactate dehydrogenase efflux assay. *J Neurosci Methods* 20: 83–90, 1987.
25. **Krainock R and Murphy S.** Heregulin upregulates the expression of nitric oxide synthase (NOS)-1 in rat cerebellar granule neurons via the ErbB4 receptor. *J Neurochem* 76: 312–315, 2001.
26. **Lafon-Cazal M, Pietri S, Culcasi M, and Bockaert J.** NMDA-dependent superoxide production and neurotoxicity. *Nature* 364: 535–537, 1993.
27. **Lei SZ, Pan ZH, Aggarwal SK, Chen HS, Hartman J, Sucher NJ, and Lipton SA.** Effect of nitric oxide production on the redox modulatory site of the NMDA receptor-channel complex. *Neuron* 8: 1087–1099, 1992.
28. **Leslie SW, Brown LM, Trent RD, Lee YH, Morris JL, Jones TW, Randall PK, Lau SS, and Monks TJ.** Stimulation of *N*-methyl-D-aspartate receptor-mediated calcium entry into dissociated neurons by reduced and oxidized glutathione. *Mol Pharmacol* 41: 308–314, 1992.
29. **Levi G, Aloisi F, Ciotti MT, and Gallo V.** Autoradiographic localization and depolarization-induced release of acidic amino acids in differentiating cerebellar granule cell cultures. *Brain Res* 290: 77–86, 1984.
30. **Lipton SA, Choi YB, Pan ZH, Lei SZ, Chen HSV, Sucher NJ, Loscalzo J, Singel DJ, and Stamler JS.** A redox-based mechanism for the neuroprotective and neurodestructive effects of nitric oxide and related nitroso-compounds. *Nature* 364: 626–632, 1993.
31. **Lu YM, Yin HZ, Chiang J, and Weiss JH.** Ca^{2+} permeable AMPA/kainate and NMDA channels: high rate of Ca^{2+} influx underlies potent induction of injury. *J Neurosci* 16: 5457–5465, 1996.
32. **Mayer ML, Westbrook GL, and Guthrie PB.** Voltage-dependent block by Mg^{2+} of NMDA responses in spinal cord neurons. *Nature* 309: 261–263, 1984.
33. **Mori H and Mishina M.** Structure and function of the NMDA receptor channel. *Neuropharmacology* 34: 1219–1237, 1995.
34. **Mosmann T.** Rapid colorimetric assay for cellular growth and survival: application to proliferation and cytotoxicity assays. *J Immunol Methods* 65: 55–63, 1983.
35. **Netzeband JG, Conroy SM, Parsons KL, and Gruol DL.** Cannabinoids enhance NMDA-elicited Ca^{2+} signals in cerebellar granule neurons in culture. *J Neurosci* 19: 8765–8777, 1999.
36. **Nicholls DG and Budd SL.** Mitochondria and neuronal glutamate excitotoxicity. *Biochim Biophys Acta* 1366: 97–112, 1998.
37. **Nowak L, Bregestovski P, Ascher P, Herbet A, and Prochiantz A.** Magnesium gates glutamate-activated channels in mouse central neurons. *Nature* 307: 462–465, 1984.
38. **Ogita K, Enomoto R, Nakahara F, Ishitsubo N, and Yoneda Y.** A possible role of glutathione as an endogenous agonist at the *N*-methyl-D-aspartate recognition domain in rat brain. *J Neurochem* 64: 1088–1096, 1995.
39. **Peng TI and Greenamyre T.** Privileged access to mitochondria of calcium influx through *N*-methyl-D-aspartate receptors. *Mol Pharmacol* 53: 974–980, 1998.
40. **Reynolds IJ and Hastings TG.** Glutamate induces the production of reactive oxygen species in cultured forebrain neurons following NMDA receptor activation. *J Neurosci* 15: 3318–3327, 1995.
41. **Stamier JS, and Singel DJ, and Loscalzo J.** Biochemistry of nitric oxide and its redox-activated forms. *Science* 258: 1898–1902, 1992.
42. **Tenneti L, D'Emilia DM, Troy CM, and Lipton SA.** Role of caspases in *N*-methyl-D-aspartate-induced apoptosis in cerebrocortical neurons. *J Neurochem* 71: 946–959, 1998.
43. **Tymianski M, Charlton MP, Carlen PL, and Tator CH.** Source specificity of early calcium neurotoxicity in cultured embryonic spinal neurons. *J Neurosci* 13: 2085–2104, 1993.
44. **Wang GJ and Thayer SA.** Sequestration of glutamate-induced Ca^{2+} loads by mitochondria in cultured rat hippocampal neurons. *J Neurophysiol* 76: 1611–1621, 1996.
45. **White RJ and Reynolds IJ.** Mitochondria accumulate Ca^{2+} following intense glutamate stimulation of cultured rat forebrain neurons. *J Physiol* 498: 31–47, 1997.
46. **Xu L, Eu JP, Meissner G, and Stamler JS.** Activation of the cardiac calcium release channel (ryanodine receptor) by poly-*S*-nitrosylation. *Science* 279: 234–237, 1998.
47. **Yan GM, Ni B, Weller M, Wood K, and Paul SM.** Depolarization or glutamate receptor activation blocks apoptotic cell death of cultured cerebellar granule neurons. *Brain Res* 656: 43–52, 1994.